

# No evidence that epilepsy impacts criticality in pre-seizure single-neuron activity of human cortex

Annika Hagemann<sup>1</sup>, Jens Wilting<sup>1</sup>, Bitu Samimizad<sup>2</sup>, Florian Mormann<sup>2</sup>, Viola Priesemann<sup>1,3\*</sup>,

**1** Max-Planck-Institute for Dynamics and Self-Organization, Göttingen, Germany

**2** Department of Epileptology, University of Bonn Medical Centre, Bonn, Germany

**3** Bernstein Center for Computational Neuroscience (BCCN) Göttingen

\*Corresponding author

viola.priesemann@ds.mpg.de

## Abstract

Epileptic seizures are characterized by abnormal and excessive neural activity, where cortical network dynamics seem to become unstable. However, most of the time, during seizure-free periods, cortex of epilepsy patients shows perfectly stable dynamics. This raises the question of how recurring instability can arise in the light of this stable default state. In this work, we examine two potential scenarios of seizure generation: (i) epileptic cortical areas might generally operate closer to instability, which would make epilepsy patients generally more susceptible to seizures, or (ii) epileptic cortical areas might drift systematically towards instability before seizure onset.

We analyzed single-unit spike recordings from both the epileptogenic (focal) and the nonfocal cortical hemispheres of 20 epilepsy patients. We quantified the distance to instability in the framework of criticality, using a novel estimator, which enables an unbiased inference from a small set of recorded neurons. Surprisingly, we found no evidence for either scenario: Neither did focal areas generally operate closer to instability, nor were seizures preceded by a drift towards instability. In fact, our results from both pre-seizure and seizure-free intervals suggest that despite epilepsy, human cortex operates in the stable, slightly subcritical regime, just like cortex of other healthy mammals.

## Author summary

In epilepsy patients, the brain regularly fails to control its activity, resulting in epileptic seizures. So far, it is not fully understood why the brains of epilepsy patients are susceptible to seizures and what the mechanism behind seizure generation is.

We investigated epilepsy from the perspective of collective neural dynamics in the brain. It has been hypothesized that epileptic seizures might be a tipping over from stable, so-called subcritical, dynamics (which are commonly found in healthy brains) to unstable, so-called supercritical dynamics. We therefore examined two potential scenarios of seizure generation: (i) epileptic brain areas might generally operate closer to instability, which would make epilepsy patients generally susceptible to seizures, or (ii) epileptic brain areas might slowly drift towards instability before seizure onset. To test these two hypotheses, we analyzed activity of single neurons recorded with micro-electrodes in epilepsy patients.

Contrary to widespread expectation, we found no evidence for either scenario, thus no evidence that epilepsy involves a transition to supercritical collective neural dynamics. In fact, our results from both seizure-free and pre-seizure intervals suggest that the human epileptic brain operates in the stable regime, just like the brains of other healthy mammals.

## Introduction

The existence of epileptic seizures suggests that cortical networks self-organize to a state that is prone to instability. Interestingly, from a computational perspective, a working point at the border to instability has advantages for information processing, because it renders a network highly sensitive to input and fosters non-stereotypical responses to stimuli [1–4]. It is therefore hypothesized that cortical networks have to strike a balance between maximizing their sensitivity and variability, while maintaining a safety margin to instability [5, 6]. Indeed, evidence is accumulating that cortical networks *in vitro* as well as in healthy, awake animals operate close to a *critical point* which marks a transition between stable (subcritical) and unstable (supercritical) dynamics [1, 2, 6–23].

Epileptic seizures have been hypothesized to reflect a transition to supercritical, unstable dynamics [24–29]. However, quantitative evidence for this hypothesis remains limited. While seizure *termination* was found to show signatures of a critical transition across different recording levels [30], recent studies on seizure *initiation* did not find consistent warning signals of a critical transition prior to seizures [31, 32]. Such inherent unpredictability is characteristic for critical systems, and may provide an explanation why reliable approaches for seizure prediction have not been established to date [33, 34].

While these past findings suggest that seizure onset might correspond to loosing the safety margin to supercriticality, it remains open whether the safety margin is in general smaller in certain areas of epileptic brains, or whether the safety margin is lost prior to seizure onset. In the first scenario, one expects the seizure onset zone (SOZ) to generally operate closer to instability, and thus a clear difference between the SOZ and the same brain area in the contra-lateral, nonfocal hemisphere (nSOZ) (Fig. 1b). In the second scenario, one expects that the distance to criticality diminishes systematically before seizure onset, making the onset predictable (Fig. 1c).

We investigated these two hypotheses using extracellular spike recordings from patients with focal epilepsy. In particular, we address two questions: (i) Does the region in which the seizures emerge, i.e. the seizure onset zone (SOZ), generally differ from the nonfocal hemisphere (nSOZ) in its distance to criticality? (ii) Does the distance to criticality change systematically prior to seizure onset? To that end, we assessed the distance to criticality based on the branching parameter  $m$  (Fig. 1a). The branching parameter  $m$  characterizes the spreading of neural activity. If  $m$  is smaller than one, one action potential (spike) on average triggers less than one action potential in the subsequent time step, and the neural network is stable (subcritical regime); if  $m$  is larger than one, runaway activity may emerge and the system is unstable (supercritical regime), and  $m = 1$  marks the transition between the two (critical state) [35, 36]. To quantify  $m$ , we made use of a novel, unbiased estimator that only requires knowing the number of spikes sampled from a small set of neurons to return a reliable estimate of the branching parameter  $\hat{m}$  [36]. Importantly, the estimator is invariant under subsampling [37], thus it can infer the propagation of activity in a network even when recording only a small fraction of all neurons [12, 38].

## Results

We estimated the distance to criticality in human MTL based on single unit activity from  $n = 20$  patients with focal epilepsy. A precise quantification of the distance to criticality has become possible with a novel, unbiased estimator [36]. The estimator had returned a branching parameter of  $m \approx 0.98$  for various different mammalian species, which corresponds to stable, slightly subcritical dynamics [12, 36]. We applied the same estimator to single unit activity in human MTL, both from the hemisphere with the seizure onset zone (SOZ), and the contra-lateral one (nSOZ).

Consistent with recent studies in awake mammals [5, 6, 12, 13, 39], we found single unit activity in human MTL to reflect dynamics close to criticality, but with a small safety margin to instability (see Fig. 1). The recorded activity  $A_t$  was vastly consistent with a branching process, as most recordings clearly showed the exponential decay that is expected for the autocorrelation functions (83 out of

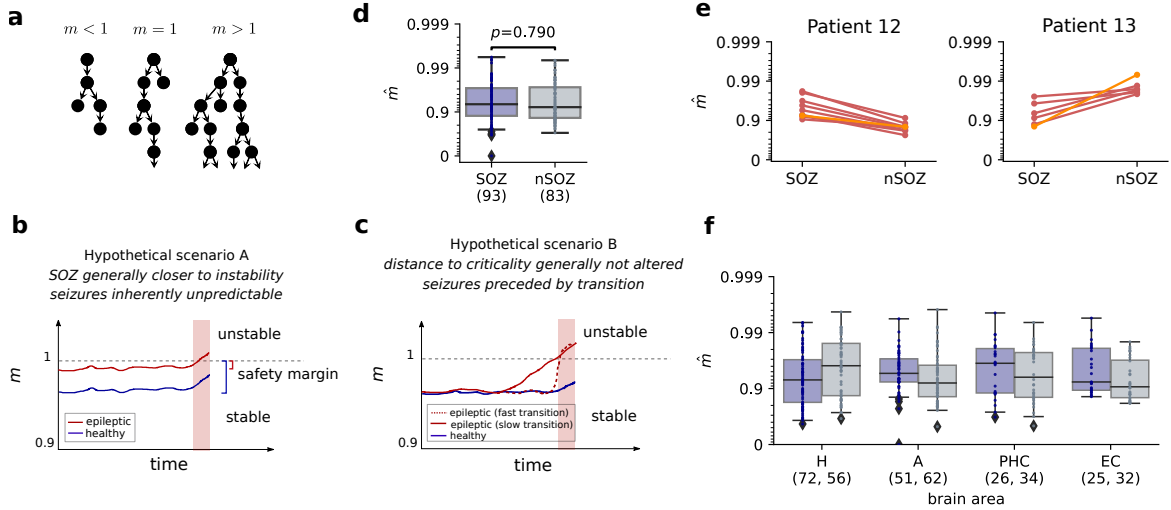


**Fig 1. Comparison of the distance to criticality between the hemisphere containing the seizure onset zone (SOZ) and the nonfocal hemisphere (nSOZ).** **a** Branching process approximation of activity propagation in the brain. Depending on the branching parameter  $m$ , dynamics are stable ( $m < 1$ ), unstable ( $m > 1$ ) or critical ( $m = 1$ ). **b, c** Hypothetical scenarios of seizure generation. The SOZ might, in general, operate closer to criticality and consequently enter the supercritical regime in an unpredictable manner because of small fluctuations (scenario A). Alternatively, dynamics might systematically drift towards instability before seizure onset. If that drift is sufficiently slow, seizures might be predictable (scenario B). **d** The branching parameter  $\hat{m}$  across recordings and patients shows no significant difference between SOZ and nSOZ (two-sided Mann Whitney-U test). **e** Estimated  $\hat{m}$  in SOZ and nSOZ for multiple recordings of two exemplary patients. While several patients showed a consistent difference between hemispheres across recordings, this difference is not predicted by the SOZ (orange: reference recording, red: pre-seizure recording, see Fig. S2 for all patients). **f** Comparison of the branching parameter  $\hat{m}$  in SOZ and nSOZ for different subregions of the MTL, (hippocampus (H), amygdala (A), parahippocampal cortex (PHC) and entorhinal cortex (EC)). None of the regions shows a significant difference between SOZ and nSOZ ( $p < 0.05/4$  required after Bonferroni correction). Box plots show median and quartiles, while whiskers extend to the rest of the distribution, except for outliers (points beyond 1.5 x interquartile range).

91 recordings in the nSOZ, 93 out of 105 recordings in the SOZ, see Fig. S1). Across subjects and recordings, the branching parameter indicated dynamics in a slightly subcritical regime, with most recordings being close to criticality ( $0.9 < m < 1$ , see Fig. 1)). Hence, our results for human MTL are consistent with those in other mammalian species, suggesting that mammalian cortex in general self-organizes to a slightly subcritical regime.

We tested the hypothesis that the seizure onset zone generally operates closer to the critical point, which would make it prone to tipping over to unstable dynamics (Fig. 1b). However, we found no significant difference between SOZ and nSOZ for  $\hat{m}$  across recordings and patients (two-sided Mann Whitney-U test,  $p \approx 0.8$ , see Fig. 1d). Within some of the patients, however, there were consistent differences in the distance to criticality between hemispheres (Figs. 1e, S2). Out of the 8 patients for whom there were sufficient recordings for a significance test, we found  $\hat{m}_{SOZ} < \hat{m}_{nSOZ}$  in 2 patients,  $\hat{m}_{SOZ} > \hat{m}_{nSOZ}$  in 2 patients and no significant difference in the remaining 4 patients. Our result thus suggests that there can be consistent differences in distance to criticality between hemispheres but that the location of the SOZ does not predict that difference.

To test whether the distance to criticality in the SOZ is only altered in specific subregions of the MTL, we analyzed the recorded activity  $A_t$  separately in each of the subregions, including amygdala, entorhinal cortex, parahippocampal cortex and hippocampus. Consistent with the above results, we found that single unit activity in all subregions reflects a subcritical regime, but none of the subregions showed a significant alteration in the SOZ, as compared to the nonfocal hemisphere (Fig. 1f). Jointly taking into account the effects of patient-ID, brain area and the location of the SOZ revealed that the variance in the branching parameter  $m$  across recordings is largely explained by patient-ID (3-way ANOVA on transformed data  $\hat{\epsilon} = \log(1 - \hat{m})$ ,  $F_{\text{patient}} = 4.0$ ,  $p_{\text{patient}} < 10^{-4}$ ), and by considerable interaction effects with patient-ID ( $F_{\text{patient:area}} = 2.27$ ,  $p_{\text{patient:area}} < 10^{-3}$ ;  $F_{\text{patient:SOZ}} = 2.5$ ,  $p \approx 0.007$ ;  $F_{\text{patient:area:SOZ}} = 2.3$ ,  $p_{\text{patient:area:SOZ}} < 10^{-4}$ ). The main effects of brain area or location of SOZ, however, were not significant. This result suggests that the distance to criticality differs mainly between individuals. *Within* patients, there can be significant differences between brain areas as well as significant differences between SOZ and nSOZ. These differences, however, do not seem to be consistent across patients.

Previous studies have reported changes in different characteristics of neural activity from seconds up to a time scale of hours prior to seizure onset [40, 41]. To investigate whether epileptic seizures are caused by systematically loosing the safety margin to supercriticality (scenario B, Fig. 1c), we estimated the branching parameter  $m(t)$  in a time-resolved manner during pre-seizure recordings (Fig. 2a, see also Fig. S5 for all patients). While the branching parameter  $\hat{m}$  showed variations over time, none of the patients consistently showed a systematic trend prior to seizure onset. As a more coarse measure, we compared the branching parameter of the first half to the second half of pre-seizure recordings (Fig. 2b). Again, we found no significant difference when approaching seizure onset, neither in the SOZ, nor in the nSOZ (Wilcoxon signed rank test,  $p \approx 0.9$ , and  $p \approx 0.8$ , respectively). Finally, we applied the same analysis to the individual subregions of MTL. None of the individual subregions showed a significant difference between the first and the second half of pre-seizure recordings (Fig. 2c). Thus, across patients and subregions of MTL, we found no evidence for dynamics approaching supercriticality during the last 10 minutes before seizure onset.

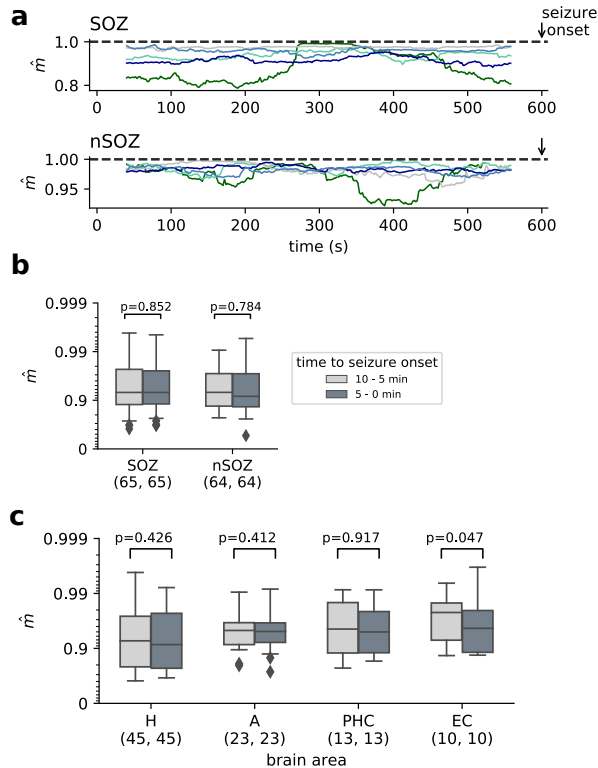


**Fig 2. No consistent change in the distance to criticality before seizure onset.** **a** Time-resolved estimation of  $\hat{m}$  for the full MTL within the last 10 min prior to seizure onset showed variability, but no consistent behavior during the last minutes before seizure onset. Plots show example traces of multiple seizures from one patient. Each trace corresponds to one pre-seizure period, shown both for the SOZ and the nSOZ. Traces of all patients and seizures shown in Fig. S5. **b** No significant difference in the distance to criticality between the last 5 min prior to seizure onset and the previous 5 min – neither in the MTL containing the SOZ, nor in the nSOZ (p-values of Wilcoxon signed rank test). **c** Separate analysis of the individual subregions of MTL. Within none of the subregions there were significant differences between the last 5 min before seizure onset and the previous 5 min. Box plots in **c** show results from the hemisphere containing the epileptic focus (SOZ).

## Discussion

We started off with the hypotheses that a brain area affected by epilepsy might (i) generally operate closer to criticality (and instability), or (ii) systematically move from the stable, subcritical to the unstable, supercritical regime before seizure onset. However, we found no evidence for either hypothesis when evaluating single unit activity of human medial temporal lobe. Instead, we found that both hemispheres, the one containing the seizure onset zone (SOZ), and the nonfocal one (nSOZ) operate in a slightly subcritical regime. Thereby our results in human medial temporal lobe are in line with those on single unit activity from multiple other mammalian species that all show reverberating, slightly subcritical dynamics [12].

We did not find any evidence for systematic transitions from the sub- to the supercritical regime before seizure onset, nor systematic differences between the SOZ and the nonfocal hemisphere. As all our recordings have been obtained during seizure-free intervals (reference or pre-seizure), this finding does not contradict the experimental evidence that epileptiform activity and seizures proper might reflect a transition to the supercritical regime [26, 27]. In the literature, the reported time window of putative pre-seizure changes varies considerably from hours over minutes to seconds [40, 42, 43]. Thus

potentially, the transition to supercriticality is so rapid that our time-resolved analysis cannot capture it (faster than the 80 seconds analysis window). For longer putative pre-seizure periods (30 minutes to 4 hours), signatures of 'critical slowing down', which are associated with transitions to supercriticality, have not been found either [32], which is consistent with our results. Thus for seizure prediction as early warning, which would be important for patients to seek a safe environment before a seizure starts, the framework of criticality has not proven useful yet.

Our analyses might miss signatures of a transition to supercritical dynamics because of not capturing the recruited set of neurons, or because single unit activity presents too fine a spatial scale. Single neuron activity before and during an epileptic seizure was shown to be highly heterogeneous, with some neurons increasing their firing rates, others decreasing, and a considerable fraction not changing at all [40]. In fact, evidence from spatially extended spike recordings from epilepsy patients suggests that there is a sharp boundary between areas with increased, hypersynchronous spiking and adjacent areas with low-level, unstructured activity during focal seizures [44]. This implies that recruitment of neurons to seizures occurs only in small areas and that single unit recordings potentially do not capture the recruited neurons [44]. In line with this idea, the study that found signatures of critical slowing during seizure *termination* found these signatures only on the more coarse recording levels (EEG, ECoG, LFP), not in multi unit activity [30]. Therefore, the sparsely recorded single unit activity may not be the ideal type of signal to identify seizure onset dynamics.

Our estimation of the distance to criticality relied on the branching process approximation. Mathematically, the branching process represents a generic model of how activity propagates in a network, but clearly, it is quite simplistic, and does not account for all the biological complexity in the brain. Instead, it returns a single parameter  $m$ , characterizing the *effective* spreading of activity. Any alteration in  $m$  may thus reflect one or a combination of mechanisms, like altered synaptic strength, excitability, or excitation-inhibition ratio.

The branching process formalism has proven powerful, because in contrast to classical approaches to estimate criticality, it is (i) invariant under subsampling, returning a reliable estimate of activity spread and stability even if only a tiny fraction of neurons is sampled [5, 36, 37, 45]; (ii) it returns a precise, quantitative estimate of the distance to criticality, which enables comparison across studies, recording conditions, brain areas, and species; and (iii) it requires comparably little data, thereby enabling our time-resolved analysis. Importantly, one finds a good match between the branching process and many experimentally observed features of cortical dynamics, like spectra, Fano factors, inter-spike interval distributions, and a clear exponential decay of the autocorrelation function [6, 12, 46, 47]. Together, these aspects clearly support the validity of the branching process approximation, making it a powerful tool to assess the stability of network dynamics.

In summary, we found no evidence for epilepsy to involve a transition towards supercritical dynamics. This finding is in line with previous studies finding no warning signals of a critical transition prior to epileptic seizures [31, 32]. However, since all the analyzed data was obtained during seizure-free intervals (pre-ictal or inter-ictal), we cannot rule out that seizure activity proper is indeed supercritical, with dynamics crossing the critical thresholds only seconds before seizure onset. Alternatively, seizure generation might be a qualitatively different process that cannot be captured by a linear stability parameter  $m$ .

## Materials and methods

### Acquisition and pre-processing of intracranial recordings

We analyzed intracranial recordings from  $n = 20$  patients with medically intractable focal epilepsy. The data was recorded at the Department of Epileptology at the University of Bonn Medical Center. For pre-surgical evaluation, patients were implanted with depth electrodes in different regions of the medial temporal lobe, including hippocampus (H), amygdala (A), parahippocampal cortex (PHC) and

entorhinal cortex (EC). All patients had given written informed consent to participate in this study, which was approved by the Medical Institutional Review Board in Bonn. Recordings were performed continuously for pre-surgical monitoring for a typical duration of 7-14 days. Data was sampled at 32 kHz and filtered between 0.1 and 9000 Hz. Spike sorting was performed using the Combinato package [48] and sorted units were classified manually as single units, multi-units, or artifacts. For further analysis, we only used spikes of identified single units and excluded artifacts and multi-units. For each patient, we analyzed one 10-minute reference recording, obtained in a seizure-free interval after the surgery, as well as several pre-ictal recordings, spanning 10 minutes prior to seizure onset. Pre-ictal recordings end at seizure onset, which was determined by two board-certified EEG readers. Patients in which the epileptic focus could not clearly be assigned to one hemisphere were excluded from the analysis. Table S1 summarizes the analyzed patients and recordings. In total, we started with 20 patients and 116 recording periods (20 reference, 96 pre-seizure). After spike-sorting and excluding recordings that did not return any single unit, 107 recording periods (20 reference, 87 pre-seizure) remained. For each of the recording periods, we obtained data from multiple subregions, which included hippocampus, amygdala, parahippocampal cortex and entorhinal cortex, but did not always cover all subregions in each patient. For the number of recordings in each hemisphere and subregion, see Suppl. 1.

### Branching process approximation

We use the branching process as a minimal model for spike propagation in the brain. The branching process is a stochastic model describing the number of active neurons  $A_t$  in discrete time bins of length  $\Delta t$ . Each active unit  $i$  at time  $t$  activates a random number  $Y_{t,i}$  of units in the subsequent time step. In addition, there is an external input  $h_t$  into the system, accounting for input from sensory modalities, from other brain areas, or spontaneous activation of individual neurons. The total number of active neurons is then given by

$$A_{t+1} = \sum_{i=1}^{A_t} Y_{t,i} + h_t. \quad (1)$$

Taking the conditional expectation value yields the autoregressive representation

$$\langle A_{t+1} | A_t = j \rangle = mj + h, \quad (2)$$

where  $m = \langle Y_{t,i} \rangle$  is the branching parameter, and  $h = \langle h_t \rangle$  is the average input.

A branching process is stable for  $m < 1$  (subcritical regime) and unstable for  $m > 1$  (supercritical regime). The critical point ( $m = 1$ ) separates the two regimes and marks the critical point of a second-order phase transition. For details, see [6, 49].

### Definition of the activity $A_t$

The activity  $A_t$  is defined as the number of active neurons in discrete time bins  $\Delta t$ . Implanted depth electrodes can, however, only record a tiny fraction of all neurons, and hence one only observes a subset of the activity  $A_t$ . Such spatial subsampling can lead to strong biases in inferred system properties [5, 11, 18, 37, 45]. However, for estimating the branching parameter  $m$ , we have developed a method that overcomes the systematic bias [36, 49]. In brief, it shows that the autocorrelation strength, which is central when inferring  $m$ , is biased by a factor  $B$ ; however, the bias factor  $B$  can be partialled out, so that we can obtain an unbiased estimate.

In the following, we thus also denote the *sampled* activity by  $A_t$ . It is defined as the number of *sampled* active neurons at time  $t$ . To obtain  $A_t$  from recorded spike times, all spikes recorded in one brain area are pooled and binned to  $\Delta t = 4$  ms time bins. The time step  $\Delta t$  was chosen to reflect the propagation time of spikes between neurons.

### Definition of the autocorrelation

To estimate  $m$ , the autocorrelation function  $C(k)$  at time lags  $k$  has to be estimated from the recorded activity  $A_t$ :

$$\begin{aligned} C(k) &= \frac{\text{Cov}[A_t, A_{t+k}]}{\text{Var}[A_t]} \\ &= \frac{\sum_{t=1}^{T-k} (A_t - \bar{A}_t)(A_{t+k} - \bar{A}_{t+k})}{\sum_{t=1}^{T-k} (A_t - \bar{A}_t)^2}, \end{aligned} \quad (3)$$

where  $\bar{A}_t$  and  $\bar{A}_{t+k}$  denote the mean activity of the original and the delayed time series, respectively, and  $T$  the duration of the recording. This definition of the autocorrelation function  $C(k)$  is equivalent to the standard definition of the Pearson correlation coefficient  $\rho_{A_t, A_{t+k}} = \frac{\text{Cov}[A_t, A_{t+k}]}{\sigma_{A_t} \sigma_{A_{t+k}}}$ , with standard deviations  $\sigma_{A_t}$ ,  $\sigma_{A_{t+k}}$ , as long as  $\{A_t\}_{t=1}^T$  is a stationary process and thereby  $\sigma_{A_t} = \sigma_{A_{t+k}}$ . If the activity  $A_t$  is consistent with a stationary process with autoregressive representation (PAR),  $C(k)$  decays exponentially [36].

### Estimation of the distance to criticality

We used our open source toolbox [38], which implements the Multistep-Regression (MR) estimator to infer the branching parameter  $m$  from spike recordings [36]. The estimator is invariant under subsampling, i.e. it yields consistent estimates for the branching parameter of the whole system even if only a small fraction of all neurons is recorded.

For a stationary branching process, it can be shown that the autocorrelation of  $A_t$  follows  $C(k) \propto m^k$ . The branching parameter  $m$  can therefore be estimated by fitting an exponential decay

$$\begin{aligned} f(k) &= Bm^k + D \\ &= B \exp(-k\Delta t/\tau) + D \end{aligned} \quad (4)$$

to the measured autocorrelation  $C(k)$ . In the last term of 4, we rewrote the autocorrelation function in terms of the intrinsic timescale  $\tau = -\Delta t / \log(m)$  [36,46]. The additional offset  $D$  in the fit function  $f(k)$  accounts for contributions with long timescales that do not decay substantially within the recording time, and it compensates for small non-stationarities in  $A_t$  [46]. The factor  $B$  is the bias factor of the autocorrelation and depends on the subsampling.

In short, given the activity  $A_t$ , estimation of  $m$  is performed in two steps [36]:

1. Compute the autocorrelation function  $C(k)$  for different time delays  $k$  (equation 3).
2. Fit an exponential decay  $f(k) = B \exp(-k\Delta t/\hat{\tau}) + D$  to the autocorrelation function to obtain an estimate for the intrinsic timescale  $\hat{\tau}$  and the branching parameter  $\hat{m} = \exp(-\Delta t/\hat{\tau})$ .

All analyses were performed using the python toolbox of the MR estimator [38]. We used time delays  $k \in [4 \text{ ms}, 1600 \text{ ms}]$ , which is on the order of several autocorrelation times of our data.

Confidence intervals of estimates for single recordings were obtained via a block bootstrap procedure: recordings were divided into segments of 20 s length and estimation was performed on random subsets of segments (see *stationarymean* method in [38]).

### Exclusion criteria of MR estimation

For reliable estimation of the branching parameter  $m$ , the data must be consistent with a stationary PAR which implies that the autocorrelation  $C(k)$  must be consistent with an exponential decay. Furthermore, reliable estimation requires a minimum number of recorded spikes, because the variance in estimates increases with decreasing number of non-zero activity entries [36]. To ensure that a given time series fulfills the requirements for reliable estimation, we implemented two consistency checks:

1. Number of non-zero time bins must be at least  $n_{A_t \neq 0} = 1000$ .
2. The exponential decay must fit the autocorrelation better than a simple linear function. (Otherwise, the data cannot be considered consistent with a stationary PAR).

If a recording was not consistent with either of these requirements, it was excluded from the analysis.

### Comparison of SOZ and nSOZ

For each recording, the spikes from the hemisphere containing the epileptic focus (SOZ) were combined and binned to a single activity time series  $A_t^{\text{SOZ}}$ . Equally, all recorded spikes from the nonfocal hemisphere (nSOZ) were binned to  $A_t^{\text{nSOZ}}$ . Estimated branching parameters  $\hat{m}$  of SOZ and nSOZ were compared by performing a two-sided Mann Whitney-U test.

The same approach was applied individually to each subregion of the MTL. In this case, spikes were binned separately for each subregion in each hemisphere and the estimated  $\hat{m}$  of SOZ and nSOZ were compared as described above.

To disentangle potential effects of patient-ID, subregion and location of the SOZ, we additionally conducted a 3-way ANOVA. As the distribution of  $\hat{m}$  was not consistent with a normal distribution, we performed the ANOVA on the logarithmic distance to criticality  $\hat{\epsilon} = \log(1 - \hat{m})$ . In addition, we performed pairwise comparisons of  $\hat{m}$  of SOZ and nSOZ in all subregions using the Mann Whitney-U test. The obtained results were consistent across the different testing procedures.

### Time-resolved estimation before seizure onset

To analyze changes in the distance to criticality  $(1 - \hat{m})$  prior to seizure onset, we applied the MR estimator with a sliding window approach. The crucial parameter to choose is the window size  $L_w$ , which represents a trade-off between sufficiently short windows for high temporal resolution, and sufficiently long windows that provide enough data for a consistent estimation. Based on the average activity and the average number of non-zero activity entries in our data, we chose a window size of  $L_w = 80$  s (see Figs. S3, S4). We used overlapping windows with a fixed window-step  $L_{\text{step}} = 2$  s. As a more coarse measure of pre-seizure changes, we splitted the pre-seizure recordings into two parts and estimated  $\hat{m}$  separately for both parts. Estimates of the first and the second part were then compared using the Wilcoxon signed rank test, where parts of the same recording were considered pairs.

## Acknowledgments

F.M. acknowledges support from the Volkswagen Foundation, the German Ministry of Education and Research (BMBF 031L0197B) and the German Research Council (DFG MO 930/8-1, SFB 1089). J.W. received support from the Gertrud- Reemtsma-Stiftung. J.W and V.P. received financial support from the German Ministry for Education and Research (BMBF) via the Bernstein Center for Computational Neuroscience (BCCN) Göttingen. A.H., J.W. and V.P. received financial support from the Max Planck Society.

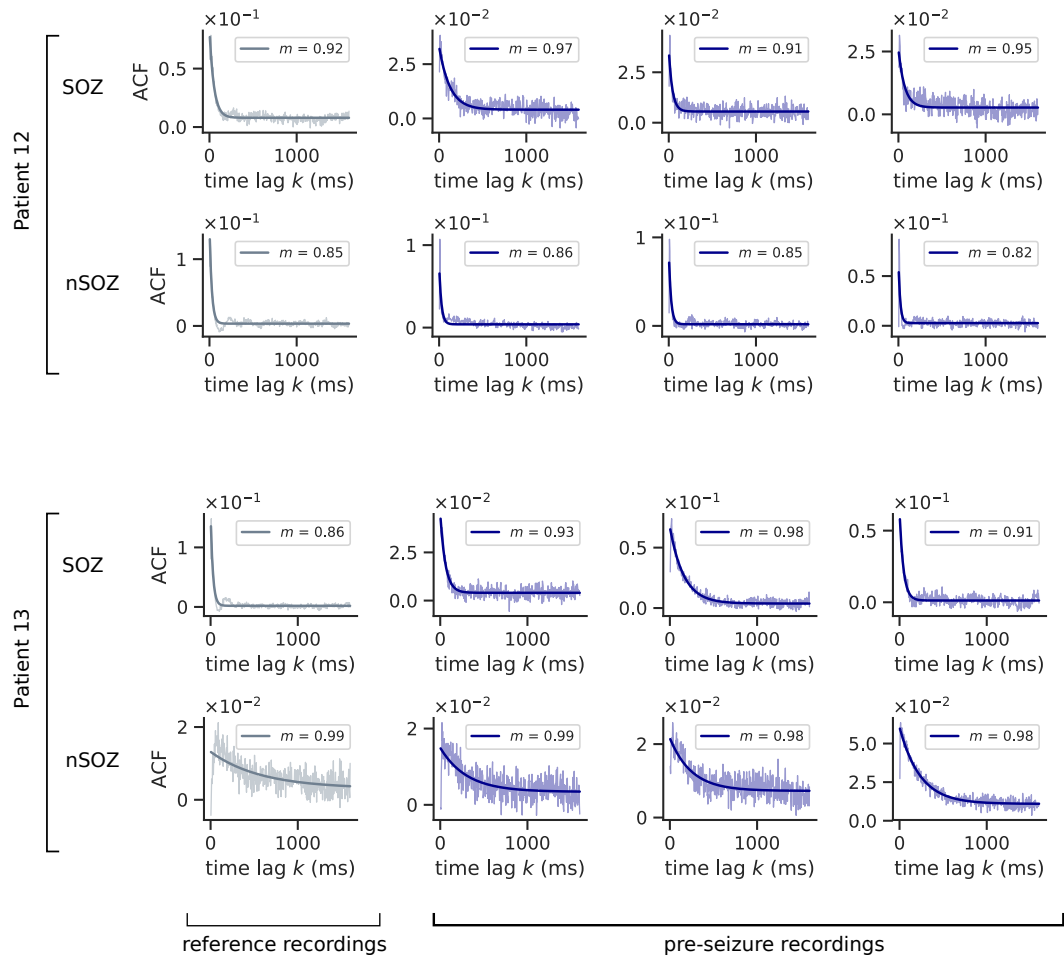
## References

1. Shew WL, Plenz D. The functional benefits of criticality in the cortex. *The neuroscientist*. 2013;19(1):88–100.
2. Haldeman C, Beggs JM. Critical Branching Captures Activity in Living Neural Networks and Maximizes the Number of Metastable States. *Physical Review Letters*. 2005;94(5):058101. doi:10.1103/PhysRevLett.94.058101.
3. Kinouchi O, Copelli M. Optimal dynamical range of excitable networks at criticality. *Nature physics*. 2006;2(5):348.
4. Bertschinger N, Natschläger T. Real-time computation at the edge of chaos in recurrent neural networks. *Neural computation*. 2004;16(7):1413–1436.
5. Priesemann V, Wibral M, Valderrama M, Pröpper R, Le Van Quyen M, Geisel T, et al. Spike avalanches in vivo suggest a driven, slightly subcritical brain state. *Frontiers in Systems Neuroscience*. 2014;8. doi:10.3389/fnsys.2014.00108.
6. Wilting J, Dehning J, Pinheiro Neto J, Rudelt L, Wibral M, Zierenberg J, et al. Operating in a Reverberating Regime Enables Rapid Tuning of Network States to Task Requirements. *Frontiers in Systems Neuroscience*. 2018;12. doi:10.3389/fnsys.2018.00055.
7. Beggs JM, Plenz D. Neuronal avalanches in neocortical circuits. *The Journal of Neuroscience: The Official Journal of the Society for Neuroscience*. 2003;23(35):11167–11177.
8. Friedman N, Ito S, Brinkman BA, Shimono M, DeVille RL, Dahmen KA, et al. Universal critical dynamics in high resolution neuronal avalanche data. *Physical review letters*. 2012;108(20):208102.
9. Zierenberg J, Wilting J, Priesemann V. Homeostatic Plasticity and External Input Shape Neural Network Dynamics. *Physical Review X*. 2018;8(3):031018. doi:10.1103/PhysRevX.8.031018.
10. Neto JP, Spitzner FP, Priesemann V. A unified picture of neuronal avalanches arises from the understanding of sampling effects. *arXiv preprint arXiv:191009984*. 2019;.
11. Wilting J, Priesemann V. 25 years of criticality in neuroscience—established results, open controversies, novel concepts. *Current opinion in neurobiology*. 2019;58:105–111.
12. Wilting J, Priesemann V. Between Perfectly Critical and Fully Irregular: A Reverberating Model Captures and Predicts Cortical Spike Propagation. *Cerebral Cortex (New York, NY: 1991)*. 2019;29(6):2759–2770. doi:10.1093/cercor/bhz049.
13. Dahmen D, Grün S, Diesmann M, Helias M. Second type of criticality in the brain uncovers rich multiple-neuron dynamics. *Proceedings of the National Academy of Sciences*. 2019;116(26):13051–13060.

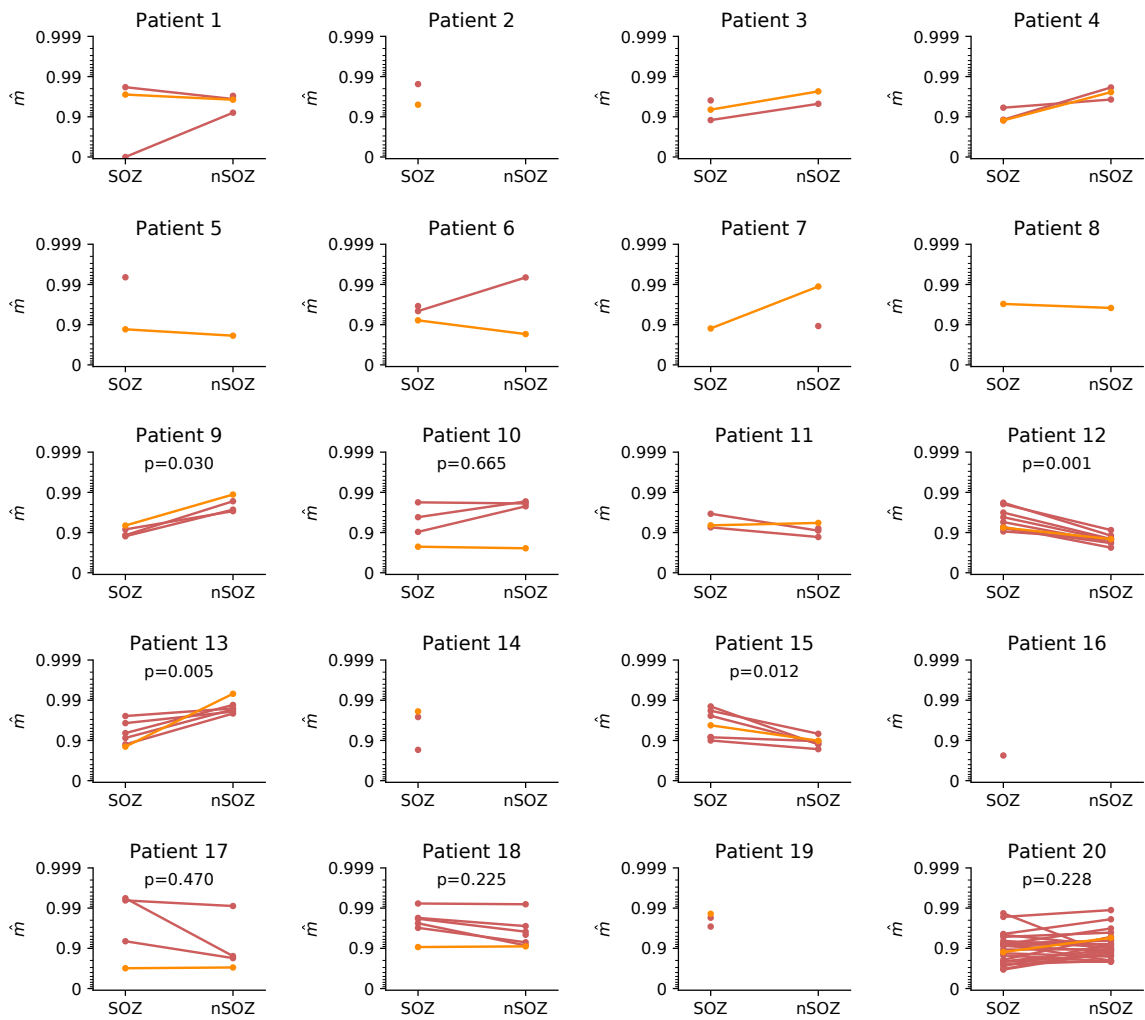
14. Munoz MA. Colloquium: Criticality and dynamical scaling in living systems. *Reviews of Modern Physics*. 2018;90(3):031001.
15. Hahn G, Petermann T, Havenith MN, Yu S, Singer W, Plenz D, et al. Neuronal avalanches in spontaneous activity in vivo. *Journal of neurophysiology*. 2010;104(6):3312–3322.
16. Cocchi L, Gollo LL, Zalesky A, Breakspear M. Criticality in the brain: A synthesis of neurobiology, models and cognition. *Progress in neurobiology*. 2017;158:132–152.
17. Aburn MJ, Holmes C, Roberts JA, Boonstra TW, Breakspear M. Critical fluctuations in cortical models near instability. *Frontiers in physiology*. 2012;3:331.
18. Ribeiro TL, Copelli M, Caixeta F, Belchior H, Chialvo DR, Nicolelis MA, et al. Spike avalanches exhibit universal dynamics across the sleep-wake cycle. *PloS one*. 2010;5(11):e14129.
19. Ribeiro TL, Ribeiro S, Belchior H, Caixeta F, Copelli M. Undersampled critical branching processes on small-world and random networks fail to reproduce the statistics of spike avalanches. *PloS one*. 2014;9(4):e94992.
20. Fagerholm ED, Scott G, Shew WL, Song C, Leech R, Knöpfel T, et al. Cortical entropy, mutual information and scale-free dynamics in waking mice. *Cerebral cortex*. 2016;26(10):3945–3952.
21. Ponce-Alvarez A, Jouary A, Privat M, Deco G, Sumbre G. Whole-brain neuronal activity displays crackling noise dynamics. *Neuron*. 2018;100(6):1446–1459.
22. Ma Z, Turrigiano GG, Wessel R, Hengen KB. Cortical circuit dynamics are homeostatically tuned to criticality in vivo. *Neuron*. 2019;104(4):655–664.
23. Marshel JH, Kim YS, Machado TA, Quirin S, Benson B, Kadmon J, et al. Cortical layer-specific critical dynamics triggering perception. *Science*. 2019;365(6453):eaaw5202.
24. Hsu D, Chen W, Hsu M, Beggs JM. An open hypothesis: is epilepsy learned, and can it be unlearned? *Epilepsy & behavior : E&B*. 2008;13(3):511–522. doi:10.1016/j.yebeh.2008.05.007.
25. Scheffer M, Bascompte J, Brock WA, Brovkin V, Carpenter SR, Dakos V, et al. Early-warning signals for critical transitions. *Nature*. 2009;461(7260):53–59. doi:10.1038/nature08227.
26. Meisel C, Storch A, Hallmeyer-Elgner S, Bullmore E, Gross T. Failure of Adaptive Self-Organized Criticality during Epileptic Seizure Attacks. *PLOS Computational Biology*. 2012;8(1):e1002312. doi:10.1371/journal.pcbi.1002312.
27. Arviv O, Medvedovsky M, Sheintuch L, Goldstein A, Shriki O. Deviations from Critical Dynamics in Interictal Epileptiform Activity. *Journal of Neuroscience*. 2016;36(48):12276–12292. doi:10.1523/JNEUROSCI.0809-16.2016.
28. Hobbs JP, Smith JL, Beggs JM. Aberrant Neuronal Avalanches in Cortical Tissue Removed From Juvenile Epilepsy Patients. *Journal of Clinical Neurophysiology*. 2010;27(6):380. doi:10.1097/WNP.0b013e3181fd8d3.
29. Yan J, Wang Y, Ouyang G, Yu T, Li Y, Sik A, et al. Analysis of electrocorticogram in epilepsy patients in terms of criticality. *Nonlinear Dynamics*. 2016;83(4):1909–1917. doi:10.1007/s11071-015-2455-9.
30. Kramer MA, Cash SS. Epilepsy as a Disorder of Cortical Network Organization , Epilepsy as a Disorder of Cortical Network Organization. *The Neuroscientist*. 2012;18(4):360–372. doi:10.1177/1073858411422754.
31. Milanowski P, Suffczynski P. Seizures Start without Common Signatures of Critical Transition. *International Journal of Neural Systems*. 2016;26(08):1650053. doi:10.1142/S0129065716500532.

32. Wilkat T, Rings T, Lehnertz K. No evidence for critical slowing down prior to human epileptic seizures. *Chaos: An Interdisciplinary Journal of Nonlinear Science*. 2019;29(9):091104. doi:10.1063/1.5122759.
33. Mormann F, Andrzejak RG, Elger CE, Lehnertz K. Seizure prediction: the long and winding road. *Brain*. 2007;130(2):314–333.
34. Kuhlmann L, Lehnertz K, Richardson MP, Schelter B, Zaveri HP. Seizure prediction — ready for a new era. *Nature Reviews Neurology*. 2018; p. 1. doi:10.1038/s41582-018-0055-2.
35. Harris TE. *The Theory of Branching Processes*. Grundlehren der mathematischen Wissenschaften. Berlin Heidelberg: Springer-Verlag; 1963. Available from: <https://www.springer.com/de/book/9783642518683>.
36. Wilting J, Priesemann V. Inferring collective dynamical states from widely unobserved systems. *Nature Communications*. 2018;9(1):2325. doi:10.1038/s41467-018-04725-4.
37. Priesemann V, Munk MH, Wibral M. Subsampling effects in neuronal avalanche distributions recorded in vivo. *BMC neuroscience*. 2009;10(1):40.
38. Spitzner FP, Dehning J, Wilting J, Hagemann A, Pinheiro Neto J, Zierenberg J, Priesemann V. Python toolbox for the multistep regression estimator; 2019. Available from: <https://github.com/Priesemann-Group/mrestimator>.
39. Tomen N, Rotermund D, Ernst U. Marginally subcritical dynamics explain enhanced stimulus discriminability under attention. *Frontiers in systems neuroscience*. 2014;8:151.
40. Truccolo W, Donoghue JA, Hochberg LR, Eskandar EN, Madsen JR, Anderson WS, et al. Single-neuron dynamics in human focal epilepsy. *Nature Neuroscience*. 2011;14(5):635–641. doi:10.1038/nn.2782.
41. Gast H, Niediek J, Schindler K, Boström J, Coenen VA, Beck H, et al. Burst firing of single neurons in the human medial temporal lobe changes before epileptic seizures. *Clinical Neurophysiology*. 2016;127(10):3329–3334. doi:10.1016/j.clinph.2016.08.010.
42. Badawy R, Macdonell R, Jackson G, Berkovic S. The peri-ictal state: cortical excitability changes within 24 h of a seizure. *Brain*. 2009;132(4):1013–1021.
43. Litt B, Lehnertz K. Seizure prediction and the pre-seizure period. *Current opinion in neurology*. 2002;15(2):173–177.
44. Schevon CA, Weiss SA, McKhann Jr G, Goodman RR, Yuste R, Emerson RG, et al. Evidence of an inhibitory restraint of seizure activity in humans. *Nature communications*. 2012;3:1060.
45. Levina A, Priesemann V. Subsampling scaling. *Nature Communications*. 2017;8:15140. doi:10.1038/ncomms15140.
46. Murray JD, Bernacchia A, Freedman DJ, Romo R, Wallis JD, Cai X, et al. A hierarchy of intrinsic timescales across primate cortex. *Nature Neuroscience*. 2014;17(12):1661–1663. doi:10.1038/nn.3862.
47. Meisel C. Antiepileptic drugs induce subcritical dynamics in human cortical networks. arXiv:190413026 [q-bio]. 2019;.
48. Niediek J, Boström J, Elger CE, Mormann F. Reliable Analysis of Single-Unit Recordings from the Human Brain under Noisy Conditions: Tracking Neurons over Hours. *PLoS ONE*. 2016;11(12). doi:10.1371/journal.pone.0166598.
49. Priesemann V, Levina A, Wilting J. Assessing Criticality in Experiments. In: *The Functional Role of Critical Dynamics in Neural Systems*. Springer; 2019. p. 199–232.

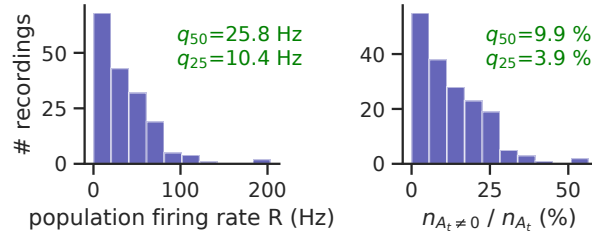
## Supplementary Material



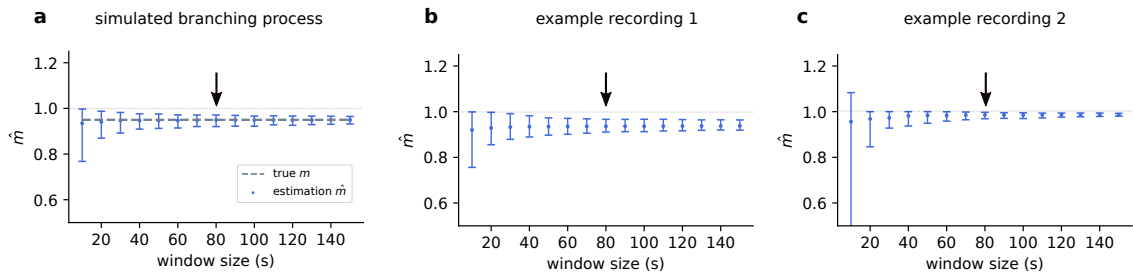
**Fig S1.** Autocorrelation functions (ACF) of single unit activity in human medial temporal lobe for two example patients. ACFs were widely consistent with exponential decays with offset (lines show the fitted exponential  $f(k) = Bm^k + D$ , where  $m$  is the estimated branching parameter). The upper row of each patient corresponds to activity in the focal hemisphere (SOZ), the lower row to the nonfocal hemisphere (nSOZ). The different plots in each row show different recordings, both reference (gray) and pre-seizure recordings (blue).



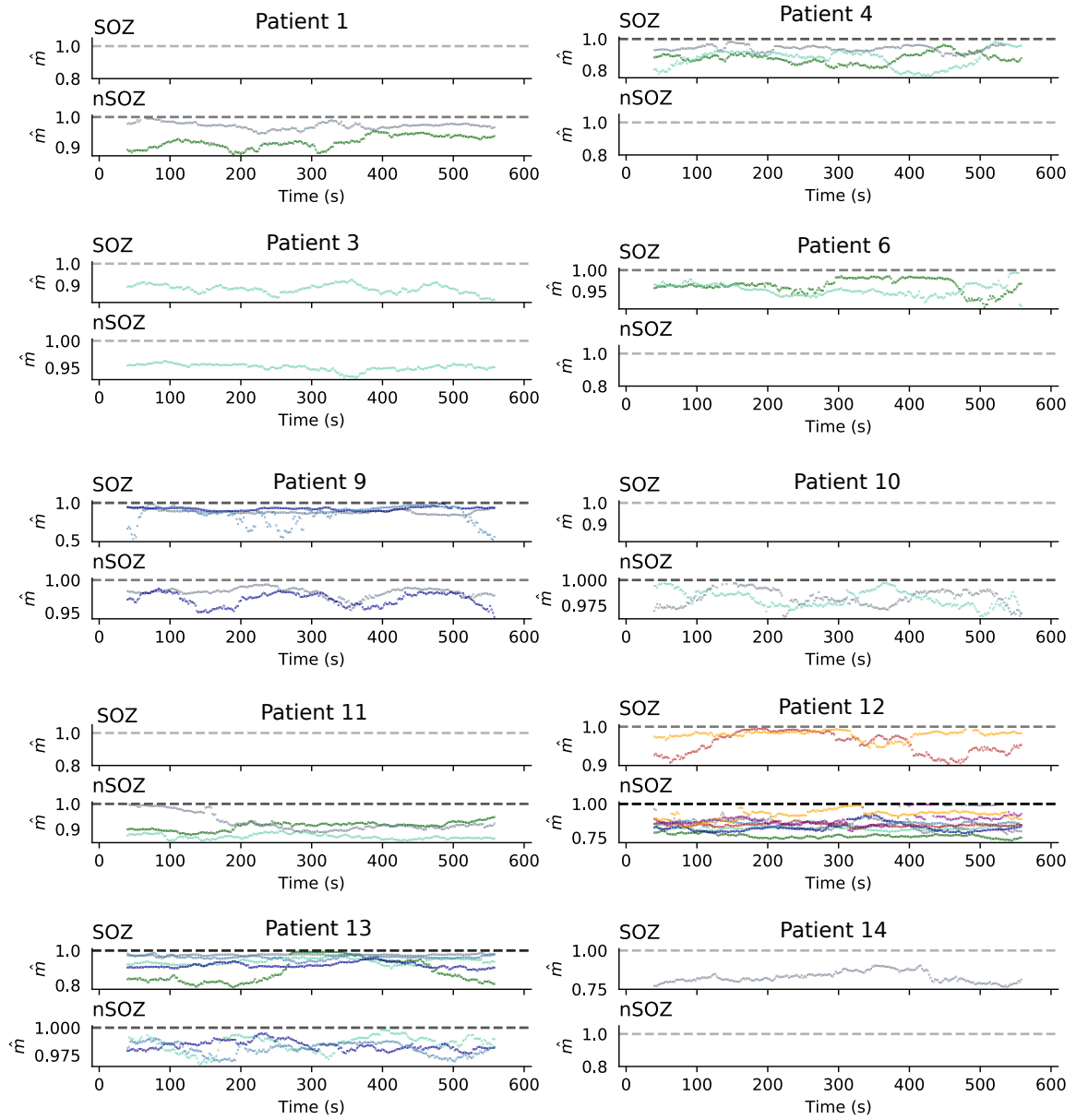
**Fig S2.** Patient-wise comparison of the branching parameter  $m$  between the hemisphere containing the seizure onset zone (SOZ) and the nonfocal hemisphere (nSOZ) for both pre-seizure recordings (red) and reference recordings (orange). While there was no consistent difference between SOZ and nSOZ *across* patients, *within* some of the patients there was a consistent trend in either direction (p-values of two-sided Mann Whitney-U test).



**Fig S3.** Average population firing rate  $R = \langle A_t \rangle_t / \Delta t$ , and number non-zero activity entries  $n_{A_t \neq 0}$ , for our dataset of pre-seizure recordings. Averages  $\langle A_t \rangle_t$  are computed over all time steps of the respective recording. Across recordings, the median population firing rate is  $q_{50} = 25.8$  Hz and the 25% quantile is  $q_{25} = 10.4$  Hz. The median fraction of non-zero activity entries is  $q_{50} = 9.9\%$ , i.e. on average, more than 90% of the time bins contain no spike.



**Fig S4.** Choice of the window size for the time-resolved estimation of the branching parameter. **a** Estimated  $\hat{m}$  as a function of the window size for simulated branching processes. Error bars are 95% confidence intervals of estimates on 500 trials. Simulation parameters were adjusted to approximately match the median values of  $\langle A_t \rangle$  and  $n_{A_t \neq 0}$  of our data set ( $m = 0.95$ ,  $\alpha = 0.004$ ,  $\Delta t = 4$  ms,  $h = 1$ ). **b, c**  $\hat{m}$  for different window sizes in two example recordings. Error bars are 95% confidence intervals of estimates from  $n=1100$  partially overlapping segments of the recording (window step size of of 400 ms). The variance of estimates increases with decreasing window size. For the results shown in Figs. S5, 2c, we chose a window size of 80 seconds (black arrow), representing a compromise between sufficiently high temporal resolution and sufficiently low variance.



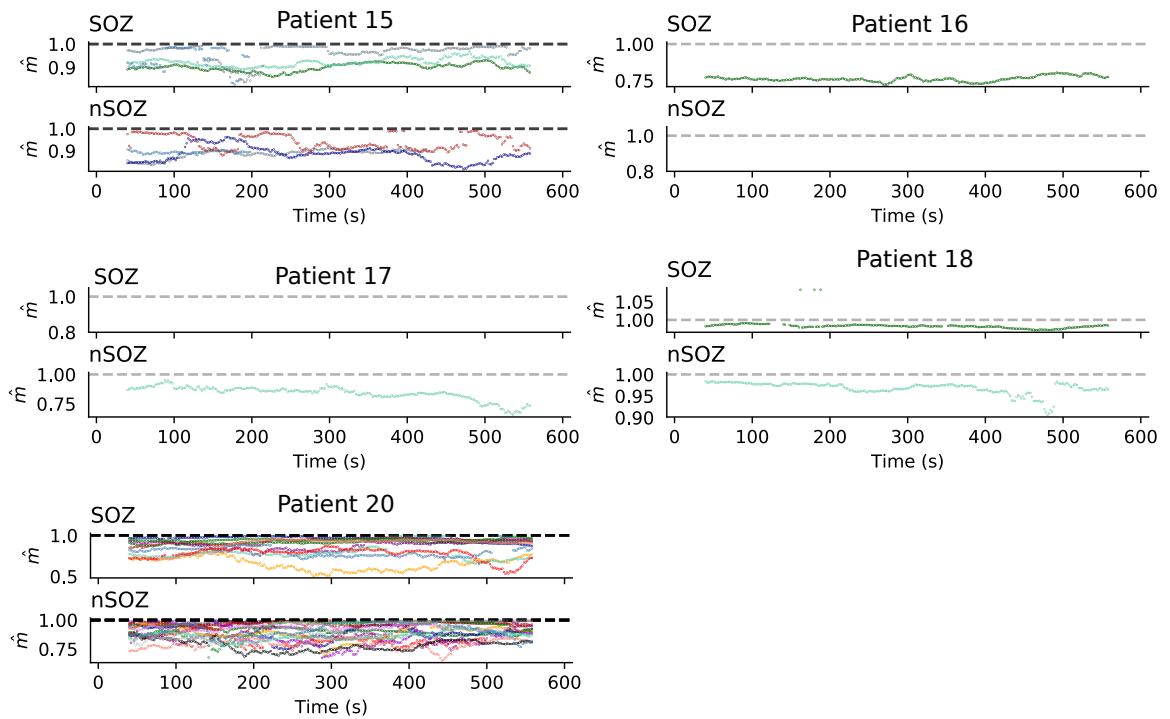


**Fig S5.** Time-resolved estimation of  $\hat{m}$  within the last 10 min prior to seizure onset for all patients and recordings. Each trace corresponds to one pre-seizure period, shown both in the SOZ and nSOZ. Seizure onset of each trace was at  $t = 600$  s and estimated  $\hat{m}$  was assigned to the middle of the respective window (window size 80 s). Recordings, in which more than 5% of segments were not consistent with the requirements for MR estimation were excluded. Note that activity enters the supercritical regime in a few segments of patient 18, but otherwise remains in the subcritical regime across patients and recordings.

# 1 Exclusion of recordings

Based on the two exclusion criteria for MR estimation, a number of intracranial recordings were excluded:

**Nonfocal hemisphere (nSOZ):** In total, out of 91 recordings from the entire MTL (16 reference, 75 pre-seizure), 4 had to be excluded because of criterion 1 and another 4 because of criterion 2, leaving a total of 83 recordings for which we could estimate the branching parameter  $m$ .

Splitting the recordings up into the different sub-regions of MTL results in a total number of recordings of  $n = 212$  ( $n_A = 68$ ,  $n_H = 71$ ,  $n_{EC} = 35$ ,  $n_{PHC} = 38$ ). After applying the exclusion criteria, we obtained to  $\tilde{n} = 184$  recordings, for which  $m$  could be estimated ( $\tilde{n}_A = 62$ ,  $\tilde{n}_H = 56$ ,  $\tilde{n}_{EC} = 32$ ,  $\tilde{n}_{PHC} = 34$ ).

**Focal hemisphere (SOZ):** In total, out of 105 recordings from the entire MTL (20 reference, 85 pre-seizure), 3 had to be excluded because of criterion 1 and another 9 because of criterion 2, leaving a total of 93 recordings for which we could estimate the branching parameter  $m$ .

Splitting the recordings up into the different sub-regions of MTL results in a total number of recordings of  $n = 228$  ( $n_A = 72$ ,  $n_H = 84$ ,  $n_{EC} = 34$ ,  $n_{PHC} = 38$ ). After applying the exclusion criteria, we obtained to  $\tilde{n} = 174$  recordings, for which  $m$  could be estimated ( $\tilde{n}_A = 51$ ,  $\tilde{n}_H = 72$ ,  $\tilde{n}_{EC} = 25$ ,  $\tilde{n}_{PHC} = 26$ ).

patient ID	location of focus	reference recordings	pre-seizure recordings	brain regions
1	L	1	3	LA, LPHC, RA, REC
2	L	1	1	LH, LEC
3	L	1	3	LH, LPHC, RH, LA, RPHC, RA
4	L	1	4	LH, LEC, RH, RA, LA, LPHC, RPHC
5	L	1	2	LH, LPHC, RH, LA, RA
6	L	1	2	LA, LH, REC, RPHC, LEC
7	R	1	1	LA, LH, RA, REC, RPHC
8	R	1	0	LA, LEC, RA, RH, REC
9	L	1	3	LA, LH, LEC, RH, REC, RPHC
10	R	1	3	LA, LH, LPHC, REC, RPHC, RH
11	L	1	3	LA, RA, RH
12	R	1	8	LA, LEC, LPHC, RA, RH, REC, RPHC, LH
13	R	1	5	LA, LH, LEC, LPHC, RA, RH, RPHC
14	L	1	3	LA, LH
15	R	1	6	LA, LH, LEC, LPHC, RA, RH, REC, RPHC
16	L	1	1	LH
17	L	1	3	LH, RA, RH, REC, RPHC, LPHC, LA, LEC
18	L	1	8	LA, LH, RA, LEC, RH, LPHC
19	L	1	3	LA, LPHC
20	L	1	25	LH, RA, RH, LA, LPHC

**Table S1.** Intracranial recordings from epilepsy patients that were analyzed in terms of the distance to criticality. Recordings span both hemispheres (left and right) and different subregions of MTL, including hippocampus (H), amygdala (A), parahippocampal cortex (PHC) and entorhinal cortex (EC). Individual recordings of the same patient can span different subsets of the listed brain areas. Numbers of recordings after spike sorting, before applying exclusion criteria of MR estimation. Dataset provided by the Department of Epileptology in Bonn.